Chemosphere 211 (2018) 254–260

Contents lists available at ScienceDirect

Chemosphere

journal homepage: www.elsevier.com/locate/chemosphere

Effects of sulfate on simultaneous nitrate and selenate removal in a hydrogen-based membrane biofilm reactor for groundwater treatment: Performance and biofilm microbial ecology

Lijie Zhou [a], Xiaoyin Xu [b, **], Siqing Xia [b, *]

[a] College of Chemistry and Environmental Engineering, Shenzhen University, Shenzhen 518060, PR China
[b] State Key Laboratory of Pollution Control and Resource Reuse, Shanghai Institute of Pollution Control and Ecological Security, College of Environmental Science and Engineering, Tongji University, 1239 Siping Road, Shanghai 200092, PR China

HIGHLIGHTS

- Sulfate had no effects on nitrate degradation and promoted Se(VI) removal in MBfR.
- High *Hydrogenophaga* was one of the contributors for efficient nitrate degradation.
- Selenate removal was relied on bacteria of *Hydrogenophaga* and *Desulfovibrionaceae*.
- Dark hydrogen oxidation was the majority of functional profile for biofilm in MBfR.

ARTICLE INFO

Article history:
Received 26 January 2018
Received in revised form
14 July 2018
Accepted 16 July 2018
Available online 23 July 2018

Handling Editor: Y. Liu

Keywords:
Hydrogen-based membrane biofilm reactor
Sulfate
Simultaneous nitrate and selenate degradation
Desulfovibrionaceae
Hydrogen oxidation

ABSTRACT

Effects of sulfate on simultaneous nitrate and selenate removal in a hydrogen-based membrane biofilm reactor (MBfR) for groundwater treatment was identified with performance and biofilm microbial ecology. In whole operation, MBfR had almost 100% removal of nitration even with 50 mg mL^{-1} sulfate. Moreover, selenate degradation increased from 95% to approximate 100% with sulfate addition, indicating that sulfate had no obvious effects on nitrate degradation, and even partly promoted selenate removal. Short-term sulfate effect experiment further showed that Gibbs free energy of reduction (majority) and abiotic sulfide oxidation (especially between sulfate and selenate) contributed to degradable performance with sulfate. Microbial ecology showed that high percentage of *Hydrogenophaga* (≥75%) was one of the contributors for the stable and efficient nitrate degradation. Chemoheterotrophy (ratio>0.3) and dark hydrogen oxidation (ratio>0.3) were the majority of functional profile for biofilm in MBfR, and sulfate led to profiles of sulfate respiration and respiration of sulfur compounds in biofilm. Additionally, no special bacteria for selenate degradation was identified in biofilm microbial ecology, and selenate degradation was relied on *Hydrogenophaga* (75% of ecology percentage with sulfate addition) and *Desulfovibrionaceae* (4% of ecology percentage with sulfate addition). But with overloading sulfate, *Desulfovibrionaceae* was prior to sulfate degradation for energy supply and thus inhibited selenate removal.

1. Introduction

As an essential trace element for human and animals, selenium (Se) frequently enters into the environment with anthropogenic activities, especially agricultural run-off, drainage of oil refineries, mining and fossil fuels combustion (Ontiveros-Valencia et al., 2016; Tokunaga and Takahashi, 2017). Previous studies (Lenz et al., 2008; Chen et al., 2017a; Wang et al., 2017) have showed that selenium has been accumulating potentially in the nature, and selenium pollution has been considered as a matter of public and scientific attention in the last decades. Selenium has been identified globally in the range of 0.01–2.0 mg kg^{-1} in soil. Hendry et al. (2015) reported that coalmine waste rock in the Elk Valley of British Columbia (Canada) had the average concentration of 3.12 mg Se

* Corresponding author.
** Corresponding author.
E-mail addresses: xiaoyinxus@gmail.com (X. Xu), siqingxia@gmail.com (S. Xia).

https://doi.org/10.1016/j.chemosphere.2018.07.092
0045-6535/

kg^{-1}, and Molnar et al. (2018) showed that some of soil with shales or sandstones contained as high as 1200 mg kg^{-1} selenium. Several incidents of selenium poisoning have been reported in Hubei (China), Shanxi (China) and Punjab (India) (Winkel et al., 2012; Zhu et al., 2017). Therefore, due to high concentration of selenium accumulation in soil, groundwater has been facing the strong potential selenium pollution. In USA, groundwater in Utah was detected to contain over 6 mg L^{-1} selenium, and over 9 mg L^{-1} selenium was identified in groundwater of Colorado (Gore et al., 2010; Ji and Wang, 2017). Selenium pollution in groundwater has become the serious problem in recent years. Furthermore, selenium is in the form of four oxidation states in aqueous solutions (−2, 0, +4 and + 6), and selenate (Se(VI)) is the most common form for selenium in the aqueous environment due to its high solubility and mobility (Constantino et al., 2017; Tokunaga and Takahashi, 2017). Moreover, because selenate also is the most toxicity selenium, the provisional guideline for selenium in drinking water of World Health Organization (WHO) is 40 μg L^{-1}, and the maximum concentration of selenium in drinking water must be below 50 μg L^{-1} (Zhu et al., 2017). In many countries, including European Union, Canada, US, China, etc., the limit for selenium, especially for selenate, is required below 10 μg L^{-1} (Xie et al., 2017; Cui et al., 2018). Consequently, selenate removal in groundwater is the hot topic for water treatment, especially in China, in recent years.

Although chemical or physical methods, such as nano zero-valent iron, M-Al double hydroxide, barite, MgO nanosheets, have been applied for selenate removal in groundwater (Constantino et al., 2017; Tokunaga and Takahashi, 2017; Xie et al., 2017; Cui et al., 2018), biological treatment is still the priority for selenate degradation because groundwater also contains high concentration of nitrate for simultaneous removal. Hydrogen-based membrane biofilm reactor (MBfR) is a technology to delivers H_2 as electron donor for bacteria by diffusion through the membrane pores to reduce oxidized contaminants (nitrate, selenate, sulfate, chromate, etc.), which thus is considered as the promising method for simultaneous nitrate and selenate removal. Zhao et al. (2013) and Xia et al. (2011) have reported that MBfR could excellently remove selenate and nitrate in the groundwater. However, high concentration of sulfate is also detected in the groundwater, and it was also figured out that sulfate, as the oxidized contaminant, presents a direct effect on simultaneous removal of nitrate and other oxidized contaminants in MBfR (Ontiveros-Valencia et al., 2014; Chen et al., 2017b). Li et al. (2017) has reported that sulfate should have a certain of effects on selenate and nitrate removal, but without further microbial ecology analysis. Ontiveros-Valencia (Ontiveros-Valencia et al., 2016) has identified biofilm microbial ecology of MBfR, but without functional profile analysis. Therefore, effects of sulfate on simultaneous nitrate and selenate removal of MBfR still need a further study.

This study aimed to further identify the effects of sulfate on simultaneous nitrate and selenate removal of MBfR, especially to identify the relationship between performance and biofilm microbial ecology. A laboratory-scale MBfR was operated with long-term and short-term experiments in this study. Degradation of nitrate, selenate and sulfate were analyzed, and consumed electron was also calculated. At last, biofilm microbial ecology and its functional profiles were detected and discussed with performance variations to get better understanding sulfate effects on simultaneous nitrate and selenate removal.

2. Materials and methods

2.1. Long-term experimental set of MBfR

A 600 mL working volume laboratory-scale MBfR (Fig. 1), which

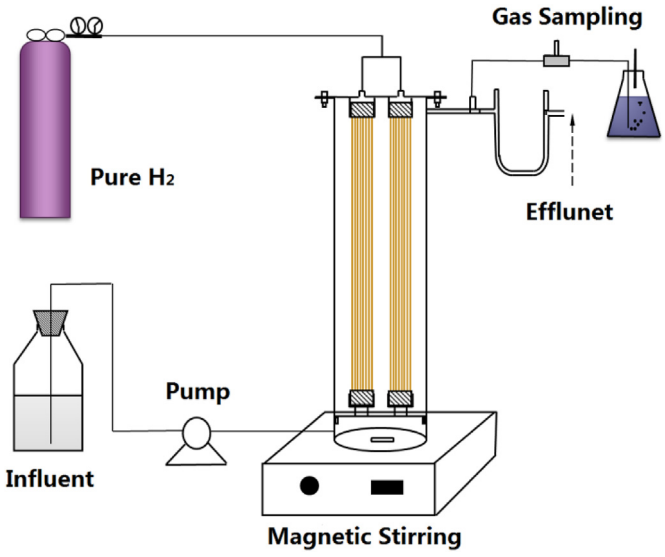

Fig. 1. A schematic of hydrogen-based membrane biofilm reactor.

was modified according to previous studies (Xia et al., 2013, 2016), was operated in this study. Two polyvinylidene difluoride (PVDF) membrane modules (Litree Company, China) were installed in the middle of reactor. Membrane module totally contained 132 fibers with membrane surface area of 990 cm^2 and pore size of 0.1 μm. Magnetic stirrer was applied for complete liquid mixture during MBfR operation. Influent flow rate was controlled with a single peristaltic pump. Biofilm formation occurred on the membrane surface, and stable pure H_2 diffused into reactor through membrane pores to provide electron for biofilm. Reactor was maintained around 24–26 °C with heating blanket and air condition during whole operation.

The influent in this study was groundwater with addition of 0.6633 mg L^{-1} $NaHCO_3$, 0.2923 mg L^{-1} KH_2PO_4, 0.01 mg L^{-1} $MgCl_2$, 0.001 mg L^{-1} $FeSO_4 \cdot 7H_2O$, 0.001 mg L^{-1} $CaCl_2 \cdot 2H_2O$, 0.013 mg L^{-1} $ZnSO_4 \cdot 7H_2O$, 0.038 mg L^{-1} H_3BO_3, 0.001 mg L^{-1} $CuCl_2 \cdot 2H_2O$, 0.004 mg L^{-1} $Na_2MoO_4 \cdot 2H_2O$, 0.004 mg L^{-1} $MnCl_2 \cdot 4H_2O$, 0.025 mg L^{-1} $CoCl_2 \cdot 6H_2O$ and 0.001 mg L^{-1} $NiCl_2 \cdot 6H_2O$ for bacterial growth according to previous literature (Xu et al., 2015). The influent was set in a 10 L glass bottle, and bubbled with pure N_2 gas for over 30 mins to maintain the redox potential of mixed liquor in MBfR around −200 mV during operation, then sealed with a rubber stopper to maintain anaerobic condition. The biofilm was inoculated from the anaerobic biomass in the anoxic tank of Quyang municipal wastewater treatment plant (WWTP). MBfR was started-up with 10 mg L^{-1} NO_3^--N and 2 mg L^{-1} Se(VI) with 5.2 h hydraulic retention time (HRT; flux rate = 1 mL $min^{-1)}$ and 40 kPa H_2 pressure to achieve steady effluence for biofilm acclimatization, then the reactor was operated for three conditions (Table 1) for over 75 days. Normally, MBfR performance could be considered as stability based on effluent conditions after approximate 5 hydraulic retention time (HRT) operation (Chung et al., 2008; Ziv-El and Rittmann, 2009), and each condition in this study was operated for over 65 HRT for stable performance.

2.2. Short-term sulfate effect experiment

After long-term experimental set, short-term sulfate effect experiment is carried out to further identify effects of sulfate, especially high concentration, on simultaneous nitrate and selenate removal in MBfR. Five sulfate concentration (0, 25, 50, 100 and

Table 1
Operational conditions of MBfR.

Stage	Time (d)	NO_3^--N (mg N L^{-1})	Se(VI) (mg L^{-1})	SO_4^{2-} (mg L^{-1})	HRT (h) Flux rate (mL min^{-1})	H_2 Pressure (kPa)
I	1st–17th	10	2	–	5.2 1.0	40
II	18th-47th	10	2	50	5.2 1.0	40
III	48th-77th	10	2	50	10.4 0.5	40

200 mg L^{-1}) were applied for MBfR with similar groundwater loading with 5 mg L^{-1} NO_3^--N and 0.25 mg L^{-1} Se(VI). In all short-term experiments, MBfR was under HRT of 5.2 h (flux rate = 1 mL min^{-1}) and 40 kPa H_2 pressure. Before each sulfate concentration experiment, MBfR was operated with the certain of condition for over 10 HRT to stabilize the performance.

2.3. DNA extraction and cloning library

Biofilm samples were collected at the end of Stage I and Stage III in the long-term experiment. For each collection, 3 pieces 10 cm hollow fibers with biofilm were firstly drawn from different locations on the membrane modules. Then, fibers would be cut into small pieces and separated from membrane surface with glass ball and 5 min ultrasonic (SK3300-35 KHz, China). Biofilm samples were washed by TENP buffer and re-suspended with a sodium phosphate buffer before DNA extraction (Xu et al., 2015). Total genomic DNA was extracted from biofilm samples with Fast DNA Spin Kit (MP Biomedicals, LLC, France) following the manufacturer's instructions. Then, genomic DNA was analyzed with complete cloning library according to reference (Zhou et al., 2016). 100 positive clones were selected for sequencing. Chimeric sequences were identified as described and excluded from subsequent analysis software (Bellerophon, Australia). All the sequences were compared to the known sequences for phylogenetic analysis. Operational taxonomic units (OTUs) were defined as groups in which the sequence similarity was more than 97%. Then the obtained representative sequences were compared to available rRNA gene sequences in GenBank using the NCBI Blast program, and further the bacterial abundance in microbial ecology of each sample was calculated based on the analyzed taxonomic data. Phylogenetic tree was analyzed with software Mega 5 (Zhou et al., 2016). To predict the function potential of bacterial community, FAPROTAX 1.1 (Louca et al., 2016) was used to get the output functional table with default settings based on the taxonomic information obtained for the sample in each stage.

2.4. Other analysis

All liquid samples were kept at 4 °C after immediate filtration with 0.22 μm polyether sulfone syringe filter (Anpel Company, Shanghai, China). Nitrate, nitrite, sulfate, selenate and selenite were measured with ion chromatograph (ICS-1000, Dionex, USA) containing an AS-20 column, an AG-20 precolumn and a 150 mg L^{-1} injection loop. S^{2-} was analyzed through methylene blue spectrophotometric method with UV-VIS spectrophotometer (4802 UV/VIS, UNICO, USA) (APHA, 1998), and was also detected and compared with ion chromatograph (ICS-1000, Dionex, USA) method (similar as the above detective condition). Dissolved oxygen (DO) concentration and pH were measured via a DO-pH-redox potential meter (HQ4d, HACH, USA). Based on the kinetic analysis for identifying the relationships among electron donor and acceptor (Ziv-El and Rittmann, 2009), consumed electron was calculated with the electron balance according to surface loadings of the electron acceptors (modulated simultaneously by varying the HRT or individually by changing the influent concentration), the effluent concentrations and removal fluxes.

3. Results and discussion

3.1. Long-term performance of MBfR

MBfR was operated under 3 stages as Table 1 showed. Fig. 2 illustrates variations of nitrate, selenate and sulfate degradation during Stage I, Stage II and Stage III. As Table 1 shows, Stage I worked as control for simulate degradation of nitrate and selenate in MBfR. Stage I (Fig. 1) shows that MBfR had approximate 100% nitrate removal and achieved about 95% selenate degradation, indicating that nitrate was the prior electron acceptor from H_2 than selenate. It was considered as the result of higher Gibbs free energy of nitrate than selenate (Table 2) (Xia et al., 2013; Li et al., 2017). When MBfR was operated with similar condition besides 50 mg L^{-1} sulfate addition (Stage II), MBfR had the similar degradable performance of nitrate and selenate as Stage I. This predicts that surfate did not have obvious effects on electron consumption of nitrate and selenate during MBfR operation. Additionally, no sulfate was removed during Stage II, which meant that nitrate and selenate achieved electron from H_2 prior to sulfate. It was because Gibbs free energy of sulfate reduction was much lower than that of nitrate and selenate reduction, especially nitrate. Moreover previous studies (Hockin and Gadd, 2003; Zhou et al., 2014; Ontiveros-Valencia et al., 2017) also reported that the incomplete sulfate reduction probably was partly because of abiotic sulfide oxidation coupled to selenite oxidation. During stage III, the influent flux rate was decreased from 1.0 to 0.5 mL min^{-1} to increase HRT of nitrate, selenate and sulfate, which meant overloading H_2 for oxidized contaminants in the influent. As Fig. 2 shows, MBfR not only had 100% nitrate removal, but also presented high degradation (approximate 100%) of selenate. Additionally, sulfate in the effluent started to decrease from about 49 mg L^{-1} to 38.5 mg L^{-1}, and S^{2-} also maintained approximately 10.4 mg L^{-1} in the effluent during Stage III, indicating that sulfate was transformed into S^{2-} with hydrogen as the electron donor.

Furthermore, this study has also calculated the consumed electrons between degradations of nitrate, selenate and sulfate. During Stage I and Stage II, consumed electron of nitrate degradation both remained around 5.2 mmol e^- day^{-1}, which meant that sulfate did not have an obvious effects on nitrate removal of MBfR. Consumed electron of selenate removal also kept stably at 1.2 mmol e^- day^{-1}. In the other hands, consumed electron of sulfate degradation was unstable (1.4 ± 0.9 mmol e^- day^{-1}) during Stage II, directly leading to poor sulfate removal. During Stage III, with over electron supply, nitrate and selenate still worked as prior electron acceptor. Consumed electron of sulfate degradation also increased from 0.9 to 4.7 mmol e^- day^{-1} with high removal efficiency. Therefore, electron consumption competition from H_2 contributed

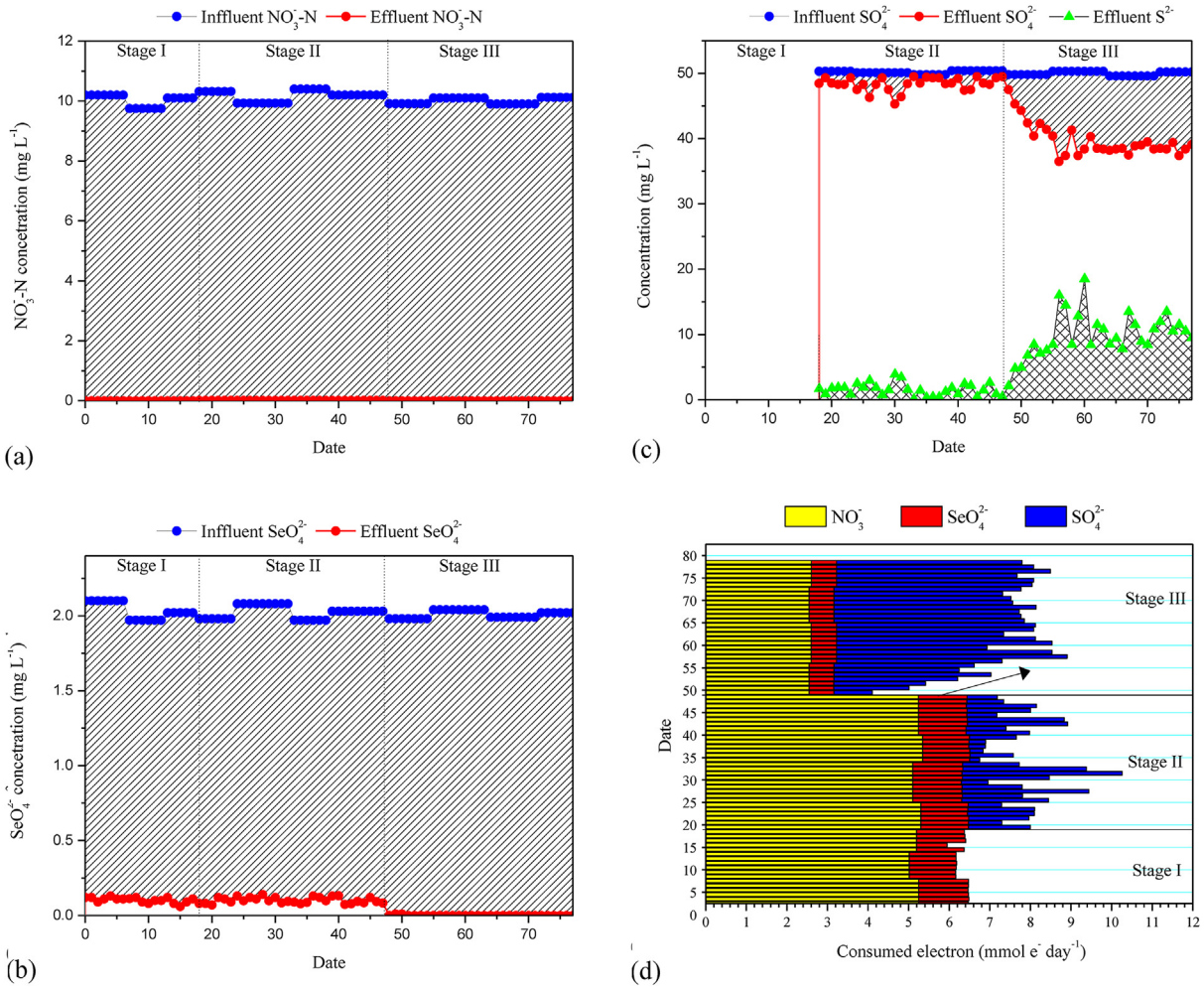

Fig. 2. Long-term performance of (a) nitrate degradation, (b) selenate degradation, (c) sulfate degradation and (d) consumed electron distribution.

Table 2
Gibbs free energy ($\triangle G_o'$) of reduction reaction for nitrate, selenate and sulfate with hydrogen as the electron donor.

Item	Reaction	$\triangle G_o'$ (kJ e^{-1})
Nitrate	$NO_3^- + 2.5H_2 + H^+ \rightarrow 0.5N_2 + 3H_2O$	−112
Selenate	$SeO_4^{2-} + 3H_2 + 2H^+ \rightarrow Se^0 + 4H_2O$	−71
Sulfate	$SO_4^{2-} + 8H_2 + 3H^+ \rightarrow HS^- + H_2O + 8H_2O$	−19

to the effects of sulfate on simultaneous nitrate and selenate removal. Previous literature (Xia et al., 2013; Ontiveros-Valencia et al., 2016; Li et al., 2017) also reported that electron competition was due to the Gibbs free energy of oxidized contaminant reduction. Consequently, sulfate did not show obvious negative effects on simultaneous nitrate and selenate removal of MBfR. Furthermore, sulfate addition even partly promoted selenate degradation.

3.2. Short-term sulfate effect experiments

For better understanding effects of sulfate, especially high concentration, on simultaneous nitrate and selenate removal, short-term sulfate effect experiments were also carried out with 25, 50, 100 and 200 mg SO_4^{2-} L^{-1}. As results of Fig. 3 and Table S1 shows, nitrate was finally transferred into N_2 without any nitrite during MBfR operation. Fig. 3(c) further presented that nitrate remained stable consumed electron of 2.6 mmol e^- day^{-1}. This indicated that nitrate had higher electron acceptability than sulfate, and thus sulfate, even with high concentration of 200 mg L^{-1}, would not have any effects on nitrate removal. Moreover, Fig. 3 also presented that most of selenate was finally removed in the MBfR with all sulfate concentrations experiments. Consequently, even with high concentration sulfate stress, MBfR still was prior to removing the nitrate and selenate in the reactor. In MBfR operation, H_2 was applied as the electron donor for biodegrading electron acceptors of nitrate, selenate and sulfate (Li et al., 2017). Thus, Gibbs free energy of reduction partly decides the completion of different electron acceptors for H_2 utilization (Chung et al., 2006; Li et al., 2014). As Table 2 shows, the Gibbs free energy of sulfate reduction ($\triangle G_o' = -19$ kJ e^{-1}) is lower than that of both nitrate removal ($\triangle G_o' = -112$ kJ e^{-1}) and selenate degradation ($\triangle G_o' = -71$ kJ e^{-1}). This means that the reduction of both nitrate and selenate compete more strongly for H_2 in MBfR operation, which answers the result of effective nitrate and selenate removal even with high sulfate stress. Additionally, little selenite ($\leq$0.02 mg L^{-1}) was detected in the effluent, and small decrease (from 0.02 to 0.01 mg L^{-1}) of selenite in the effluent was showed with sulfate advance, indicating sulfate promoting the selenium removal of MBfR, which was similar as the result of Section 3.1. Previous literatures (Hockin and Gadd, 2003; Zhou et al., 2014; Ontiveros-Valencia et al., 2017) reported that the abiotic sulfide oxidation

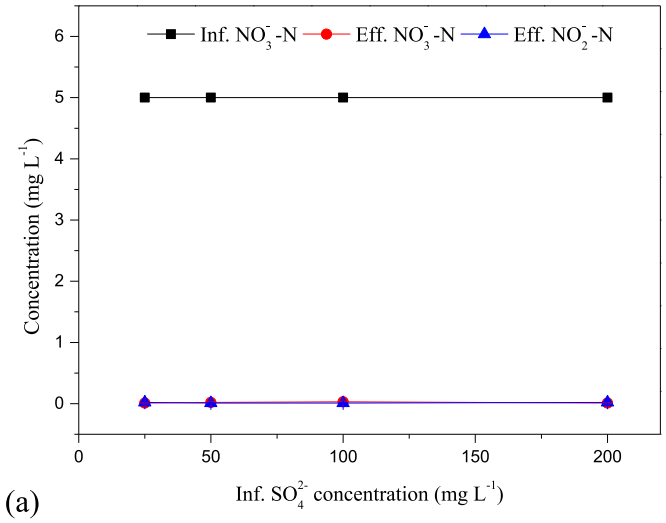

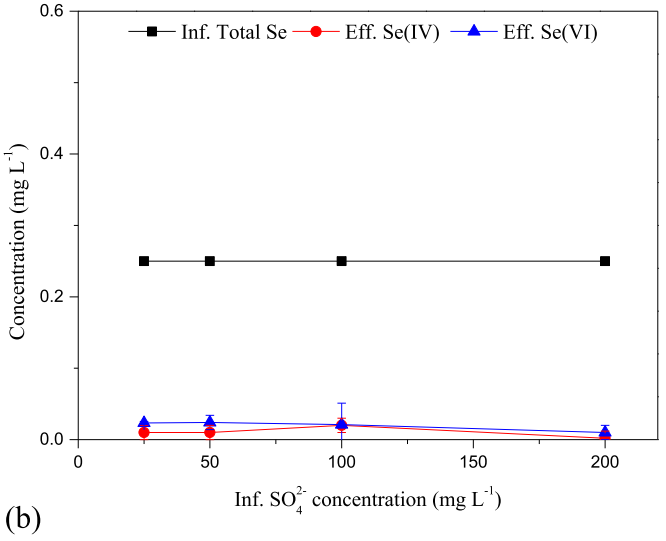

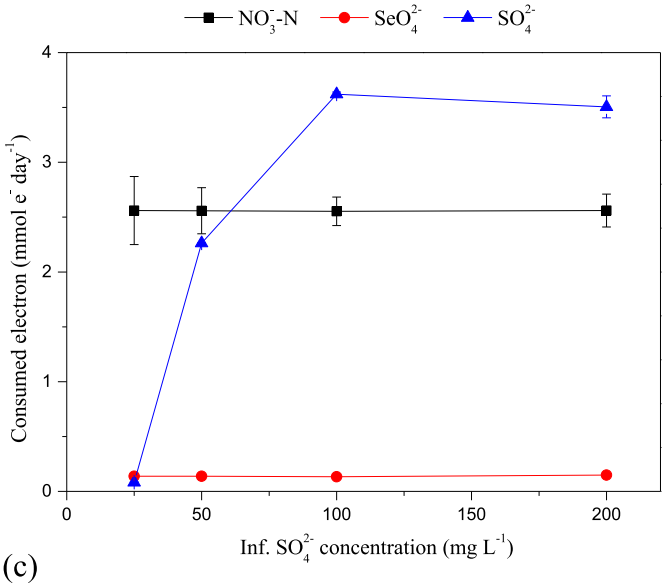

Fig. 3. Short-term sulfate effect experiment result: (a) nitrate degradation, (b) selenate degradation, (c) consumed electron distribution.

would couple to selenite oxidation during MBfR operation as follow:

$$SO_4^{2-} + 9H^+ + 8e^- \rightarrow HS^- + 4H_2O \quad (1)$$

$$HS^- \rightarrow S^0 + H^+ + 2e^- \quad (2)$$

$$SeO_3^{2-} + 6H^+ + 4e^- \rightarrow Se^0 + 3H_2O \quad (3)$$

Normally, sulfate reduction was the combination of eq. (1) and eq. (2). But, eq. (3) of half reaction for selenate reduction and eq. (1) could be combined for abiotic sulfide oxidation as:

$$SeO_3^{2-} + 2HS^- + 4H^+ \rightarrow Se^0 + 2S^0 + 3H_2O \quad (4)$$

Hockin and Gadd (2003) reported that this was a strongly exothermic reaction and is thermodynamically favored over competing reactions. Therefore, sulfate partly promoted selenate degradation. In addition, microbial ecology also plays a significant role in biodegrading electron acceptors of nitrate, selenate and sulfate (Ontiveros-Valencia et al., 2016), and thus microbial ecology would be discussed in the following section. Moreover, Table S1 and Fig. 3(c) show that electron acceptability of sulfate increased obviously from 0.1 to 3.6 mmol e^- day^{-1}. Therefore, sulfate in high concentration partly promoted selenate degradation.

3.3. Biofilm microbial ecology in MBfR

The microbial ecology of biofilm in MBfR (Fig. 4) was identified at the end of operation of Stage I and Stage III. Fig. S1 (Supporting Information, SI) shows the phylogenetic tree (100 randomly selected clones) of biofilm at the end of Stage I and Stage III (the microbial ecology of inoculating anaerobic biomass showed in Fig. S1). Biofilm microbial ecology during Stage I (Fig. 4) mainly included *β-Proteobacteria* (88.6%), *γ-Proteobacteria* (3.51%), *α-Proteobacteria* (0.88%) and *Flavobacteriia* (7.02%). Stage III had the similar biofilm microbial ecology (*β-Proteobacteria* (79.1%), *γ-Proteobacteria* (10.0%), *Sphingobacteriales* (10.9%), etc.) as Stage I. This similarity means that sulfate only led to slight shift of microbial ecology. In addition, the majority of biofilm community (86%) during Stage I was belonged to *Hydrogenophaga*, which was reported as H_2 utilization bacteria (Zhang et al., 2009; Zhao et al.,

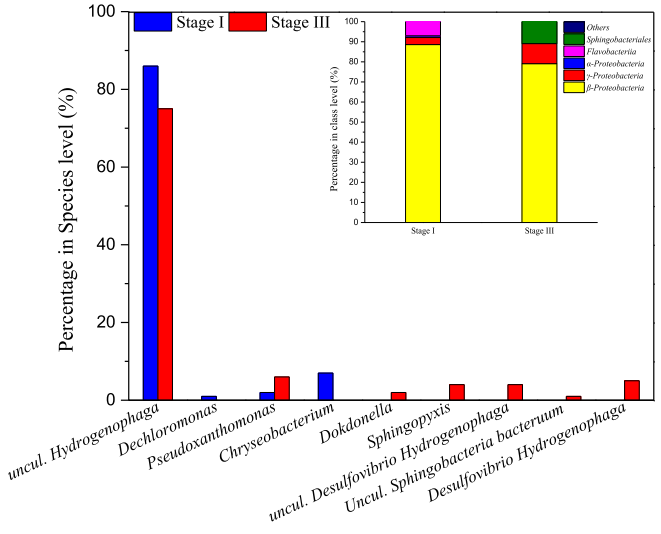

Fig. 4. Microbial ecology of biofilm in MBfR during Stage I and Stage III.

2011). The high percentage of *Hydrogenophaga* should contribute to the excellent nitrate degradation, even with sulfate addition. Consequently, sulfate would not induce any obvious effects on nitrate removal during MBfR operation. Moreover, as Fig. 4 shows, sulfate addition led to the percentage increase of *Desulfovibrionaceae*, which was sulfate reduction bacteria. It indicated that sulfate caused microbial ecology shift of biofilm, and parts of sulfate was reduced into S^{2-} in MBfR (Fig. 2(c)). Furthermore, 16s rRNA data of biofilm (Fig. 5) predicted that functional profiles of biofilm in MBfR mainly contained chemoheterotrophy, dark hydrogen oxidation, respiration of sulfur compounds and sulfate respiration. Chemoheterotrophy and dark hydrogen oxidation were the majority of functional profile for biofilm during whole MBfR operation, because bacteria in biofilm, especially *Hydrogenophaga*, utilized hydrogen as electron donor for energy supply of microbial growth. In addition, functional profiles also showed that sulfate respiration and respiration of sulfur compounds increased from 0 to 0.07%, explaining sulfate removal and increasing S^{2-} in the effluent during Stage III.

In the other hands, in both of phylogenetic trees showed no special bacteria for selenate degradation. Actually, Sabaty et al. (2001) reported that non-specific selenate and selenite reduction were carried out by some denitrifying microorganisms through the nitrate and nitrite reduction pathways. Thus, high percentage of *Hydrogenophaga* maintained the high removal of selenate during MBfR operation (Stage I). Additionally, *Desulfomicrobium norvegicum*, bacteria of *Desulfovibrionaceae*, was reported to degrade selenate with simultaneous sulfate reduction in the previous literature (Hockin and Gadd, 2003). In the latter studies (Lenz et al., 2009; Truong et al., 2013), more and more bacteria of *Desulfovibrionaceae* was identified to possess the selenate biodegradability. Ontiveros-Valencia et al. (2016) also figured out *Desulfovibrionaceae* in the biofilm microbial ecology of similar MBfR reactor with selenate, nitrate, sulfate and others oxidized contaminants. Thus, parts of sulfate reduction bacteria are considered to be capable of selenate reduction together with sulfate reduction (Subedi et al., 2017). It is because sulfate has been identified as a contributor for differences in Se accumulation and varies considerably in concentration between sites, in part as a result of anthropogenic activities (Lo et al., 2015). Therefore, with sulfate addition, selenate degradation of MBfR was not obviously inhibited, and the percentage increase of *Desulfovibrionaceae* could promote the selenate removal.

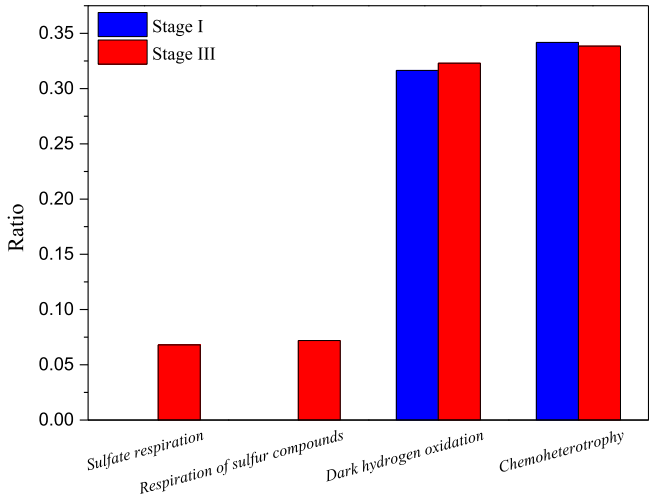

Fig. 5. Functional profiles of biofilm microbial ecology during Stage I and Stage III. [a] Ratio= (bacterial abundances with this functional profile)/(total bacterial abundances).

Based on above results, the Gibbs free energy of oxidized contaminant reduction and the abiotic sulfide oxidation (especially between sulfate and selenate) both contributed to effects of sulfate on simultaneous nitrate and selenate removal in MBfR. Additionally, as data of microbial ecology shows, high percentage of *Hydrogenophaga* was one of the contributor for the stable and efficient nitrate degradation. Furthermore, no special bacteria for selenate degradation was identified in the microbial ecology, and selenate degradation was relied on the bacteria of *Hydrogenophaga* and *Desulfovibrionaceae*. Consequently, selenate degradation was partly promoted with 50 mg L^{-1} sulfate addition because of *Desulfovibrionaceae* increase. But when sulfate was with obviously higher concentration than selenate, *Desulfovibrionaceae* was prior to sulfate degradation because of bacterial metabolism, and thus selenate removal would be inhibited.

4. Conclusions

Effects of sulfate on simultaneous nitrate and selenate removal in MBfR was studied. Sulfate had no obvious effects on nitrate degradation during MBfR operation due to the advantages of Gibbs free energy and microbial ecology for nitrate removal. In the other hand, sulfate promoted selenate degradation with 50 mg L^{-1}, which was because *Desulfovibrionaceae* was capable of selenate reduction together with sulfate reduction. But sulfate showed the inhibition for selenate removal when sulfate was obviously higher than selenate. It was because *Desulfovibrionaceae* was prior to sulfate degradation due to the bacterial metabolism.

Acknowledgments

This work is funded by “Project 51708362 and 51678422 supported by National Natural Science Foundation of China”, “State Key Laboratory of Pollution Control and Resource Reuse Foundation (NO. PCRRF17025)” and “New Teacher Natural Science Research Project of Shenzhen University (85303-00000135)”.

Appendix A. Supplementary data

Supplementary data related to this article can be found at https://doi.org/10.1016/j.chemosphere.2018.07.092.

References

APHA, 1998. Standard Methods for the Examination of Water and Wastewater, twentieth ed. American Pubilc Health Association, Washington, DC, USA.
Chen, S.S., Sun, Y.Q., Tsang, D.C.W., Graham, N.J.D., Ok, Y.S., Feng, Y.J., Li, X.D., 2017a. Insights into the subsurface transport of As(V) and Se(VI) in produced water from hydraulic fracturing using soil samples from Qingshankou Formation, Songliao Basin, China. Environ. Pollut. 223, 449–456.
Chen, X.M., Liu, Y.W., Peng, L., Ni, B.J., 2017b. Perchlorate, nitrate, and sulfate reduction in hydrogen-based membrane biofilm reactor: model-based evaluation. Chem. Eng. J. 316, 82–90.
Chung, J., Ahn, C.H., Chen, Z., Rittmann, B.E., 2008. Bio-reduction of N-nitrosodimethylamine (NDMA) using a hydrogen-based membrane biofilm reactor. Chemosphere 70, 516–520.
Chung, J., Nerenberg, R., Rittmann, B.E., 2006. Bio-reduction of soluble chromate using a hydrogen-based membrane biofilm reactor. Water Res. 40, 1634–1642.
Constantino, L.V., Quirino, J.N., Monteiro, A.M., Abrao, T., Parreira, P.S., Urbano, A., Santos, M.J., 2017. Sorption-desorption of selenite and selenate on Mg-Al layered double hydroxide in competition with nitrate, sulfate and phosphate. Chemosphere 181, 627–634.
Cui, W.W., Li, P., Wang, Z.M., Zheng, S.L., Zhang, Y., 2018. Adsorption study of selenium ions from aqueous solutions using MgO nanosheets synthesized by ultrasonic method. J. Hazard Mater. 341, 268–276.
Gore, F., Fawell, J., Bartram, J., 2010. Too much or too little? A review of the conundrum of selenium. J. Water Health 8, 405–416.
Hendry, M.J., Biswas, A., Essilfie-Dughan, J., Chen, N., Day, S.J., Barbour, S.L., 2015. Reservoirs of selenium in coal waste rock: Elk Valley, British Columbia, Canada. Environ. Sci. Technol. 49, 8228–8236.
Hockin, S.L., Gadd, G.M., 2003. Linked redox precipitation of sulfur and selenium

under anaerobic conditions by sulfate-reducing bacterial biofilms. Appl. Environ. Microbiol. 69, 7063–7072.
Ji, Y.X., Wang, Y.T., 2017. Selenium reduction by batch cultures of Escherichia coli strain EWB32213. J. Environ. Eng. 143.
Lenz, M., Enright, A.M., O'Flaherty, V., van Aelst, A.C., Lens, P.N.L., 2009. Bioaugmentation of UASB reactors with immobilized Sulfurospirillum barnesii for simultaneous selenate and nitrate removal. Appl. Microbiol. Biotechnol. 83, 377–388.
Lenz, M., Van Hullebusch, E.D., Hommes, G., Corvini, P.F.X., Lens, P.N.L., 2008. Selenate removal in methanogenic and sulfate-reducing upflow anaerobic sludge bed reactors. Water Res. 42, 2184–2194.
Li, H.X., Lin, H., Xu, X.Y., Jiang, M.M., Chang, C.C., Xia, S.Q., 2017. Simultaneous bioreduction of multiple oxidized contaminants using a membrane biofilm reactor. Water Environ. Res. 89, 178–185.
Li, H.X., Zhang, Z.Q., Xu, X.Y., Liang, J., Xia, S.Q., 2014. Bioreduction of para-chloronitrobenzene in a hydrogen-based hollow-fiber membrane biofilm reactor: effects of nitrate and sulfate. Biodegradation 25, 205–215.
Lo, B.P., Elphick, J.R., Bailey, H.C., Baker, J.A., Kennedy, C.J., 2015. The effect of sulfate on selenate bioaccumulation in two freshwater primary producers: a duckweed (Lemna minor) and a green alga (Pseudokirchneriella subcapitata). Environ. Toxicol. Chem. 34, 2841–2845.
Louca, S., Parfrey, L.W., Doebeli, M., 2016. Decoupling function and taxonomy in the global ocean microbiome. Science 353, 1272–1277.
Molnar, A., Feigl, G., Trifan, V., Ordog, A., Szollosi, R., Erdei, L., Kolbert, Z., 2018. The intensity of tyrosine nitration is associated with selenite and selenate toxicity in Brassica juncea L. Ecotoxicol. Environ. Saf. 147, 93–101.
Ontiveros-Valencia, A., Penton, C.R., Krajmalnik-Brown, R., Rittmann, B.E., 2016. Hydrogen-Fed biofilm reactors reducing selenate and sulfate: community structure and capture of elemental selenium within the biofilm. Biotechnol. Bioeng. 113, 1736–1744.
Ontiveros-Valencia, A., Tang, Y.N., Krajmalnik-Brown, R., Rittmann, B.E., 2014. Managing the interactions between sulfate-and perchlorate-reducing bacteria when using hydrogen-fed biofilms to treat a groundwater with a high perchlorate concentration. Water Res. 55, 215–224.
Ontiveros-Valencia, A., Zhou, C., Ilhan, Z.E., de Saint Cyr, L.C., Krajmalnik-Brown, R., Rittmann, B.E., 2017. Total electron acceptor loading and composition affect hexavalent uranium reduction and microbial community structure in a membrane biofilm reactor. Water Res. 125, 341–349.
Sabaty, M., Avazeri, C., Pignol, D., Vermeglio, A., 2001. Characterization of the reduction of selenate and tellurite by nitrate reductases. Appl. Environ. Microbiol. 67, 5122–5126.
Subedi, G., Taylor, J., Hatam, I., Baldwin, S.A., 2017. Simultaneous selenate reduction and denitrification by a consortium of enriched mine site bacteria. Chemosphere 183, 536–545.
Tokunaga, K., Takahashi, Y., 2017. Effective removal of selenite and selenate ions from aqueous solution by barite. Environ. Sci. Technol. 51, 9194–9201.
Truong, H.Y.T., Chen, Y.W., Belzile, N., 2013. Effect of sulfide, selenite and mercuric mercury on the growth and methylation capacity of the sulfate reducing bacterium Desulfovibrio desulfuricans. Sci. Total Environ. 449, 373–384.
Wang, D., Zhou, F., Yang, W.X., Peng, Q., Man, N., Liang, D.L., 2017. Selenate redistribution during aging in different Chinese soils and the dominant influential factors. Chemosphere 182, 284–292.
Winkel, L.H.E., Johnson, C.A., Lenz, M., Grundl, T., Leupin, O.X., Amini, M., Charlet, L., 2012. Environmental selenium Research: from microscopic processes to global understanding. Environ. Sci. Technol. 46, 571–579.
Xia, S.Q., Li, H.X., Zhang, Z.Q., Zhang, Y.H., Yang, X., Jia, R.Y., Xie, K., Xu, X.T., 2011. Bioreduction of para-chloronitrobenzene in drinking water using a continuous stirred hydrogen-based hollow fiber membrane biofilm reactor. J. Hazard Mater. 192, 593–598.
Xia, S.Q., Liang, J., Xu, X.Y., Shen, S., 2013. Simultaneous removal of selected oxidized contaminants in groundwater using a continuously stirred hydrogen-based membrane biofilm reactor. J. Environ. Sci. 25, 96–104.
Xia, S.Q., Xu, X.Y., Zhou, C., Wang, C.H., Zhou, L.J., Rittmann, B.E., 2016. Direct delivery of CO2 into a hydrogen-based membrane biofilm reactor and model development. Chem. Eng. J. 290, 154–160.
Xie, Y.K., Dong, H.R., Zeng, G.M., Zhang, L.H., Cheng, Y.J., Hou, K.J., Jiang, Z., Zhang, C., Deng, J.M., 2017. The comparison of Se(IV) and Se(VI) sequestration by nanoscale zero-valent iron in aqueous solutions: the roles of solution chemistry. J. Hazard Mater. 338, 306–312.
Xu, X.Y., Xia, S.Q., Zhou, L.J., Zhang, Z.Q., Rittmann, B.E., 2015. Bioreduction of vanadium (V) in groundwater by autohydrogentrophic bacteria: mechanisms and microorganisms. J. Environ. Sci. 30, 122–128.
Zhang, Y.H., Zhong, F.H., Xia, S.Q., Wang, X.J., Li, J.X., 2009. Autohydrogenotrophic denitrification of drinking water using a polyvinyl chloride hollow fiber membrane biofilm reactor. J. Hazard Mater. 170, 203–209.
Zhao, H.P., Ilhan, Z.E., Ontiveros-Valencia, A., Tang, Y.N., Rittmann, B.E., Krajmalnik-Brown, R., 2013. Effects of multiple electron acceptors on microbial interactions in a hydrogen-based biofilm. Environ. Sci. Technol. 47, 7396–7403.
Zhao, H.P., Van Ginkel, S., Tang, Y.N., Kang, D.W., Rittmann, B., Krajmalnik-Brown, R., 2011. Interactions between perchlorate and nitrate reductions in the biofilm of a hydrogen-based membrane biofilm reactor. Environ. Sci. Technol. 45, 10155–10162.
Zhou, C., Vannela, R., Hyun, S.P., Hayes, K.F., Rittmann, B.E., 2014. Growth of desulfovibrio vulgaris when respiring U(VI) and characterization of biogenic uraninite. Environ. Sci. Technol. 48, 6928–6937.
Zhou, L.J., Zhao, M., Feng, L., Wang, X., Xu, X.Y., Xia, S.Q., 2016. Performance and bacterial community structure of an anoxic/oxic membrane bioreactor treating anaerobically digested piggery wastewater. Desalination Water Treat. 57, 28581–28591.
Zhu, L., Zhang, L.J., Li, J., Zhang, D., Chen, L.H., Sheng, D.P., Yang, S.T., Xiao, C.L., Wang, J.Q., Chai, Z.F., Albrecht-Schmitt, T.E., Wang, S., 2017. Selenium sequestration in a cationic layered rare earth hydroxide: a combined batch experiments and EXAFS investigation. Environ. Sci. Technol. 51, 8606–8615.
Ziv-El, M.C., Rittmann, B.E., 2009. Systematic evaluation of nitrate and perchlorate bioreduction kinetics in groundwater using a hydrogen-based membrane biofilm reactor. Water Res. 43, 173–181.